Article

Dextran–Lipase Conjugates as Novel Tools for Low Molecular Weight Ligand Immobilization in Microarray Development.

Sonia Herranz, Marzia Marciello, David Olea, Margarita Hernandez, Concepcion Domingo, Marisela Vélez, Levi A Gheber, José Manuel Guisán, and Maria Cruz Moreno-Bondi

Anal. Chem., **Just Accepted Manuscript** • DOI: 10.1021/ac400631t • Publication Date (Web): 02 Jul 2013

Dextran–Lipase Conjugates as Novel Tools for Low Molecular Weight Ligand Immobilization in Microarray Development.

Sonia Herranz[†], Marzia Marciello[‡], David Olea[‡], Margarita Hernández[#], Concepción Domingo[#], Marisela Vélez[‡,¥], Levi A. Gheber[§], Jose M. Guisan[‡,], María Cruz Moreno-Bondi[†,*]*

[†]Department of Analytical Chemistry, Faculty of Chemistry, Complutense University, 28040 Madrid (Spain). [‡]Department of Biocatalysis, Institute of Catalysis and Petroleochemistry–CSIC, 28049 Cantoblanco (Madrid, Spain). [#]Instituto de Estructura de la Materia–CSIC, 28006 Madrid (Spain). [¥]Instituto Madrileño de Estudios Avanzados en Nanociencia, 28049 Cantoblanco (Madrid, Spain). [§]Department of Biotechnology Engineering, Ben-Gurion University of the Negev, 84105 Beer Sheva (Israel).

KEYWORDS Dextran–lipase conjugates, Array biosensor, Microcystins, Fluoroimmunoassay, Evanescent wave.

ABSTRACT The development of effective array biosensors relies heavily on careful control of the density of surface immobilized ligands on the transducing platform. This paper describes the synthesis of new dextran–lipase conjugates of use for immobilizing low molecular weight haptens onto glass planar waveguides for immunosensor development. The conjugates were synthesized by immobilizing bacterial thermoalkalophilic lipases (BTL2) on agarose macroporous beads, followed by covalent coupling to dextran networks of variable molecular weight (1.5–40 kDa). The chimeras were immobilized via nonspecific hydrophobic interactions onto glass planar waveguides modified with 1,1,1,3,3,3-hexamethyldisilazane to obtain highly ordered and homogeneous molecular architectures as confirmed by Atomic Force Microscopy (AFM). Microcystin-LR (MCLR) was covalently bound to the dextran–BTL2 conjugates. The usefulness of this approach to immunosensor development was demonstrated by determining amounts of MCLR down to a few picograms per liter with an automated array biosensor and

evanescent wave excitation for fluorescence measurements of attached DyLight649-labeled secondary antibody. Modifying BTL2 with dextrans of an increased molecular weight (>6 kDa) provided surfaces with an increased loading capacity that was ascribed to the production of three-dimensional surfaces by effect of the analyte binding deep in the volume leading to expanded dynamic ranges (0.09–136.56 ng L^{-1}), lower LODs (0.007 ± 0.001 ng L^{-1}) and also lower IC_{50} values (4.4 ± 0.7 ng L^{-1}). These results confirm the effectiveness of our approach for the development of high performance biosensing platforms.

INTRODUCTION

Microarray technology has recently gained increasing popularity in many fields including disease fingerprinting, drug screening, toxicity assessment, cancer therapeutics and clinical diagnostics.[1–3] Use of these analytical tools has been promoted by their affording rapid screening and identification of a large number of specific analytes in small sample volumes in a single measurement, which reduces reagent consumption and assay costs relative to conventional techniques.

Glass microscope slides are the most common substrates for microarray fabrication by virtue of their low cost, fluorescent background, stability to high temperatures and stringent washing, and amenability to chemical functionalization.[4] Despite the wide commercial availability of surface modified glass slides for arraying purposes, substrate functionalization remains a critical step in microarray fabrication.[5] In addition, the availability of immobilization methods allowing array substrate reuse is bound to reduce production costs.[6]

Glass substrates functionalized with silane derivatives for further covalent attachment of the target molecule usually provide planar 2D surfaces typically exhibiting good accuracy and reliability, but also, often, low loading capacities and poor signal detection capabilities. These limitations can be partially overcome by using glass slides modified with pseudo-3D layers of materials such as dextrans, polyacrylamide gels[7,8] or agarose[9,10] that can be further modified with appropriate linkers for attachment of ligand molecules. These methodologies, which provide increased binding capacity and sensitivity, are now commercially available. However, alternative methods are still required to simplify array fabrication and expand the range of available immobilized molecules (particularly as regards low molecular weight ligands).[11,12]

In previous work, we developed immunosensors based on various transduction schemes for detecting microcystins (MCs) in environmental waters.[13,14] We found hapten immobilization onto the chip surface and homogeneity of the receptor layer to be critical in biosensor development; in fact, both factors strongly affect sensitivity, and also nonspecific binding when complex sample matrices are involved.

This paper reports a novel approach to the development of evanescent wave microarray immunosensors based on dextran–BTL2 conjugates that are retained via nonspecific hydrophobic interactions onto microscope glass slides for the covalent immobilization of microcystin LR (MCLR). Effective BTL2 modification with the polysaccharide network was confirmed by Raman and FTIR spectra. The surface of the planar waveguides after conjugate immobilization and the different immunoassay steps was characterized by AFM. The resulting microarray was used for the sensitive, selective, rapid detection of MCs by competitive inhibition and fluorescence detection.[14–16] The influence of the dextran molecular weight on the microarray sensitivity and analytical response range was examined, and measurements were correlated with the formation of 2D or 3D immobilization layers on the sensing platform.

EXPERIMENTAL SECTION

Materials. *Geobacillus thermocatenulatus* (BTL2), which was expressed in *E. coli*, was produced and purified as described elsewhere.[17] Sucrose monolaurate, hydroxylamine hydrochloride, 1-ethyl-3-(dimethylaminopropyl) carbodiimide (EDC), ethylenediamine (EDA), *N*-hydroxysuccinimide (NHS), 2-(*N*-morpholino)ethanesulfonic acid hydrate (MES), 1H,1H,2H,2H-perfluorooctyltrichlorosilane (FOTS), 1,1,1,3,3,3-hexamethyldisilazane (HMDS), dimethyldimethoxysilane (DMDMS), D-biotin, sodium hydrogen carbonate, sodium borohydride, *p*-nitrophenyl butyrate (p-NPB) and dextrans of molecular weight 1.5–40 kDa were obtained from Sigma (St. Louis, MO, USA). HPLC-grade methanol, toluene and hexane were supplied by Panreac Quimica S.A. (Barcelona, Spain). Octyl sepharose™ was purchased from GE Healthcare (Uppsala, Sweden).

Microcystin LR (MCLR), microcystin RR (MCRR), microcystin YR (MCYR), microcystin RR desmethylated (dm-MCRR) and monoclonal MC10E7 mouse IgG antibodies raised against MCs (anti-MC Ab) were supplied by Alexis (Läufelfingen, Switzerland). IgG fraction monoclonal mouse anti-biotin and DyLight649-conjugated affinity purified rabbit anti-mouse IgG (labeled Ab) were purchased from Jackson ImmunoResearch (West Grove, PA,

USA). Biotin and MC stock solutions (1 mg mL^{-1}) were prepared in dimethyl sulfoxide (DMSO) and stored at –20 ºC. MC standard solutions for calibration were prepared on a daily basis by diluting the stock solutions in phosphate buffered saline (PBS, 20 mM, pH 7.4) containing 0.05% Tween 20 and 0.3% powder nonfat milk (PBSTM, carrier buffer). Water was purified with a Milli-Q system (Millipore, Bedford, MA). All other chemicals used were analytical reagent-grade. Borosilicate microscope slides for use as planar waveguides were purchased from Thomas Scientific (Swedesboro, NJ, USA).

Synthesis of aminated dextran–lipase conjugates. An amount of 1 g of BTL2-octyl (1–1.5 mg BTL2 per gram of octyl sepharose) was suspended in 9 mL of 1 M EDA (pH 4.75) containing 10 mM EDC and allowed to stand for 1.5 h under gentle stirring (Figure 1Sa, Supporting Information). The suspension was then filtered and the support (aminated BTL2-octyl) washed with water and dried under vacuum. Oxidized dextran was covalently linked to aminated lipase (33.4 mg mL^{-1}, pH 7; 9 mL per gram of aminated BTL2-octyl) for 1.5 h. The dextran was aminated by reaction with EDA (200 mM, pH 7.2) for 2 h, followed by addition of $NaHCO_3$ (final concentration 50 mM, pH 10) and solid sodium borohydride (final concentration 10 mg mL^{-1}) and 2 h stirring. The support was filtered and washed with excess water. The aminated dextran-BTL2 conjugate was then desorbed from the octyl sepharose support by resuspension in 10 mL of 1–2% (v/v) sucrose monolaurate in phosphate buffer (PB, 5 mM, pH 7.0) at 25 ºC for 1 h. Enzymatic activity was evaluated by measuring the increase in absorbance at 348 nm produced by the release of *p*-nitrophenol in the BTL2-catalyzed hydrolysis of 0.4 mM pNPB in 25 mM PB, pH 7 at 25 ºC. Desorption yields spanned the range 37–40% for all dextrans except that of 40 kDa (16%) (RSDs 5 - 8%) . Finally, the supernatant was filtered and sucrose monolaurate hydrolyzed with *Thermomyces lanuginosa* lipase (TLL) previously immobilized onto glyoxyl-agarose,[18] and removed by dialysis against water. Aminated dextran–BTL2 conjugates were lyophilized and stored in a dry atmosphere at 4 ºC until use. The amount of amino groups present in each conjugate was evaluated qualitatively by reacting it with 2,4,6-

trinitrobenzenesulfonate and measuring the resulting absorbance at 335 nm. Concentrations ranged from 0.13 to 0.18 μmol mg^{-1}.[20]

Raman and FTIR characterization. Raman spectra were obtained on a Bruker MultiRaman FT-Raman spectrometer equipped with a 1064 nm Nd:YAG laser excitation system and a liquid N_2 refrigerated high sensitivity Ge detector. A total of 400 scans at 8 cm^{-1} intervals were performed. Infrared spectra were acquired with a Smiths Detection IlluminatIR FT–IR microspectrometer equipped with an MCT detector and mounted on the Leica microscope of a Renishaw RM2000 Confocal Raman system. An All Reflecting Objective (ARO) was used for this purpose. Spectral resolution was 8 cm^{-1} and the acquisition time 2 min. All samples were lyophilized prior to analysis.

Biosensor development. *Instrumentation.* Fluorescent images were obtained with a Leopard Array Biosensor (Hanson Technologies, Carlisle, PA, USA), which is a commercial version of an NRL Array Biosensor prototype[15,16] and described elsewhere.[14]

Antigen immobilization onto the sensing surface. The glass microscope slides used as waveguides were cleaned by immersion in a 10% KOH solution in methanol (1 h), washed with deionized water and air dried. After cleaning, the slides were functionalized with FOTS (2% in anhydrous toluene, 2 h), DMDMS (2% in anhydrous toluene, 2 h) or HMDS (0.4 M silane in anhydrous hexane, overnight) under argon. Finally, the functionalized slides were rinsed three times with toluene or hexane as required and stored in anhydrous solvent (hexane or toluene) at 4ºC until use.

Aminated dextran–BTL2 conjugates were hydrophobically adsorbed by using a 15-channel PDMS patterning gasket placed over the functionalized waveguide. A 0.5 mg mL^{-1} conjugate solution in 10 mM PB (0.15 M NaCl, pH 7.0) was injected into each channel. After 30 min of incubation at room temperature (RT), the channels were unloaded and flushed with 0.5 mL of PB. MCLR was immobilized onto the dextran network by injecting a 20 μg mL^{-1} MCLR solution containing 100 mM EDC and 50 mM NHS in MES buffer (0.05 M, pH 6.0) into each channel (Figure 1Sb). After at least 4 h incubation, the channels were unloaded and flushed with

0.5 mL of MES buffer. An MES buffer solution (0.05 M, pH 6.0) containing 20 μg mL^{-1} MCLR or 60 μg mL^{-1} biotin plus 100 mM EDC and 50 mM NHS was patterned as negative and positive control, respectively. Additional, control channels were used to directly immobilize MCLR onto silanized surfaces in the absence of aminated dextran–BTL2 conjugate. The patterned slides were blocked in PBS containing 0.5% Tween 20 and 3% nonfat milk for 2h, rinsed with deionized water, dried under argon and either used immediately or stored at 4 ºC.

Assay protocol. The measuring principle of the assay was competitive inhibition between MCLR immobilized onto the chip surface and MCs present in the sample for a limited number of antibody (Ab) binding sites.

A volume of 390 μL of MCLR standard solution (in PBSTM) was mixed with 10 μL of Abs solution (anti-MC and anti-biotin Abs, 4 μg mL^{-1} in PBSTM). After pre-incubation at RT for 5 min, the mixture was incubated over the sensor surface for 20 min. Next, the channels were rinsed (2 × 0.8 mL PBSTM, 1 mL min^{-1}) and a solution containing 10 μg mL^{-1} labeled Ab in PBSTM was incubated for 20 min in order to reveal surface bound Abs. Unbound labeled Ab was removed by rising with 0.8 mL of PBSTM (4 ×, 1 mL min^{-1}). The slide was then imaged and fluorescence intensities were extracted. Finally, the sensor surface was regenerated by flowing a 50 mM NaOH solution (0.8 mL, 1 mL min^{-1}). A whole cycle, including chip regeneration, took 60 min.

Intensity data was then extracted from the CCD images and normalized as described elsewhere.[14] The normalized response was plotted against the MCLR concentration on a logarithmic scale, and the experimental data was fitted to the following four-parameter sigmoidal logistic equation:

$$Normalized\ signal = \frac{A_{\max} - A_{\min}}{1 + \left(\frac{[MCLR]}{IC_{50}} \right)^{b}} + A_{\min} \qquad (1)$$

where A_{max} is the asymptotic maximum (*viz*., the maximum signal in the absence of MCLR); b and IC_{50} are the slope of the curve and analyte concentration, respectively, at the

inflection point; and A_{min} is the asymptotic minimum. The limit of detection (LOD) was calculated as the MCLR concentration where Ab binding to immobilized MCLR was inhibited by 10%, and the dynamic range (DR) of the method as the MCLR concentrations providing a normalized signal from 20 to 80% A_{max}.

Analysis of water samples. Tap water samples were collected in plastic bottles previously rinsed with ultrapure water. The pH and ionic strength of the samples was adjusted by addition of PBSTM to a final buffer concentration of 20 mM and they were stored at 4 ºC until analysis. The samples were then filtered through a 0.45 μm nylon membrane (Whatman, Maidstone, UK) to remove suspended matter and analyzed in sextuplicate. Additionally, water samples free of MCs were spiked with increasing concentrations of MCLR to evaluate the matrix effect on the developed immunoassay.

Atomic Force Microscopy characterization. A model 5500 microscope from Agilent Technologies (Santa Clara, CA, USA) was used for AFM imaging. Measurements were made under ambient conditions in the dynamic mode, using Olympus rectangular silicon nitride cantilevers (RC800PSA, 100 × 20 μm) with a spring constant of 0.38 N m^{-1}, an estimated tip radius of 20 nm and a resonant frequency close to 70 kHz. The scanning rate was *ca.* 1.5 Hz. All images were second order flattened in order to correct for image "bow" due to nonlinearity in the piezoelectric scanner response. Surface root mean square roughness, R_q, was evaluated with the software Picoimage, from Agilent Technologies, in at least five different 2 × 2 μm^2 scans for each sample following removal of artifacts and averaging.

RESULTS AND DISCUSSION

Synthesis and characterization of dextran–lipase conjugates. Conjugates were synthesized by using the enzyme lipase BTL2 from *Bacillus thermocatenulatus* as protein carrier [Protein Data Base (PDB) code 2w22]. The choice of BTL2 was based on its stability at high temperatures, in alkaline media and in organic solvents, which allows this enzyme to be chemically modified and conjugated to polymeric networks.[19] The synthetic procedure involved immobilizing BTL2 onto

a commercial octyl sepharose support; the solid phase reaction used was intended to facilitate functionalization of the enzyme without affecting the hydrophobic pocket responsible for its catalytic activity, and also adsorption onto hydrophobic substrates. The modified enzyme retained more than 80% of its catalytic activity.

The dextran–BTL2 conjugates thus obtained were characterized by Raman and FTIR spectroscopies, and the results compared to those for unmodified BTL2. Figure 1a shows the FTIR spectrum for BTL2. As can be seen, the spectral region from 1900 to 1200 cm^{-1} contained the main protein absorption bands for peptide group vibrations, namely: amide I (1700–1600 cm^{-1}), which is mainly due to C=O stretching; amide II (1580–1510 cm^{-1}), due to N–H bending and a contribution of C–N stretching; and a weaker amide III band (1400–1200 cm^{-1}) due to N–H bending, and C–C_α and C–N stretching vibrations. The 1200–900 cm^{-1} region exhibited a weak absorption signal due to protein associated sugar chains.[21]

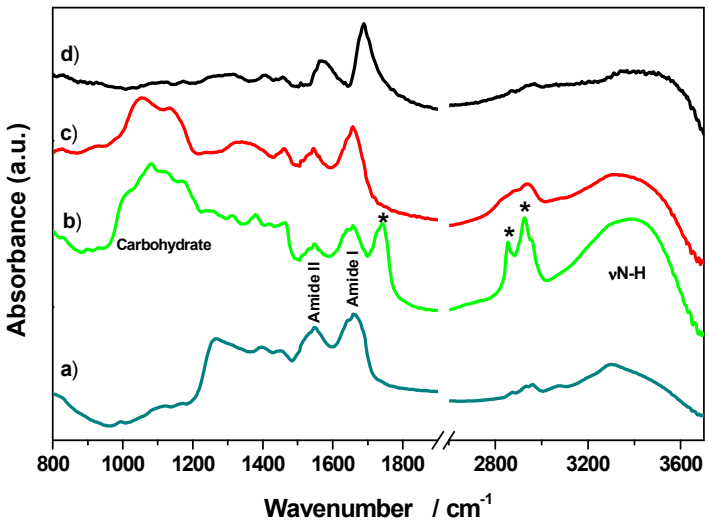

Figure 1. FTIR spectra for (a) BTL2, (b) aminated dextran–BTL2 conjugate, (c) aminated dextran–BSA conjugate and (d) BSA. (*) Sucrose laurate bands.

As confirmed by the IR and Raman spectra, the conjugates, which were desorbed from the octyl sepharose support with sucrose laurate, contained some laurate. The strongest laurate

infrared absorption (and Raman) bands by far were those in the C–H stretching region around 2900 cm^{-1}, with the typical spectral profile for alkyl chains,[22] followed by the C=O stretching band at *ca.* 1750 cm^{-1} in the infrared region. The presence of sucrose laurate residues in the samples was clearly apparent from the C=O stretching IR band at 1750 cm^{-1} and the Raman band at 1730 cm^{-1}; these bands typically appear in the 1700–1800 cm^{-1} region, where proteins and dextrans exhibit no signal. On the other hand, laurate exhibits much stronger Raman scatter than do proteins and polysaccharides such as dextran; therefore, the presence of laurate —even in trace amounts— in the conjugates produced strong enough bands to virtually conceal the Raman signals for the protein and polysaccharide.

Based on the previous results, we hypothesized that the dextran might have conjugated to BTL2 much like a protein of similar characteristics such as Bovine Serum Albumin (BSA). This hypothesis was checked by using an aminated dextran–BSA conjugate in a homogeneous phase to avoid sucrose laurate. Figures 1d, 1c and 1b show the FTIR spectra for BSA, the aminated dextran–BSA conjugate and the aminated dextran–BLT2 conjugate, respectively.

The FTIR spectra for dextrans are characterized by a strong band in the 900–1200 cm^{-1} region known as the "carbohydrate band".[23,24] Dextran derivatives (oxidized, aminated dextrans) essentially exhibit the same FTIR spectra in the fingerprint spectral region below 1800 cm^{-1}, with weak characteristic bands corresponding to various functionalities (e.g., the absorption band around 1730 cm^{-1} associated to C=O bond stretching of aldehyde groups in the oxidized dextran or a peak around 1665 cm^{-1} corresponding to stretching of the hydrazide carbonyl group in the aminated dextran).[25,26]

The aminated dextran–BTL2 conjugate contained residual sucrose laurate, labeled with an asterisk in Figure 1b. Binding of the dextran backbone to BSA (or BTL2) increased signal intensity in the aliphatic C–H stretching region (3000 cm^{-1}) and carbohydrate region (900–1200 cm^{-1}), consistent with previous results for collagen–dextran blends.[23]

Also consistent with previous results for gelatin–polysaccharide complexes,[27] formation of the protein–polysaccharide complexes increased the signals in the 900–1200 cm^{-1} region and

caused small shifts in the protein Amide I and Amide III bands, as well as in the carbohydrate peak around 1010 cm^{-1}. The presence of secondary amine groups strengthened amine N–H stretching vibrations (3300–3500 cm^{-1}). The medium–weak band for amine C–N stretching vibrations in the 1130– 1190 cm^{-1} region overlapped with the strongest bands for dextran. In conclusion, the IR spectra were consistent with the formation of aminated dextran–BSA and aminated dextran–BTL2 conjugates spectrally similar to other glycosylated lipases.[28]

As can be seen from Figures 2a and 2b, the Raman spectrum for BTL2 —after subtraction of the sucrose laurate spectrum— and that for BSA were very similar. Figure 2 also shows the spectra for the dextran (e) and aminated dextran (d), as well as the aminated dextran–BSA conjugate (c).

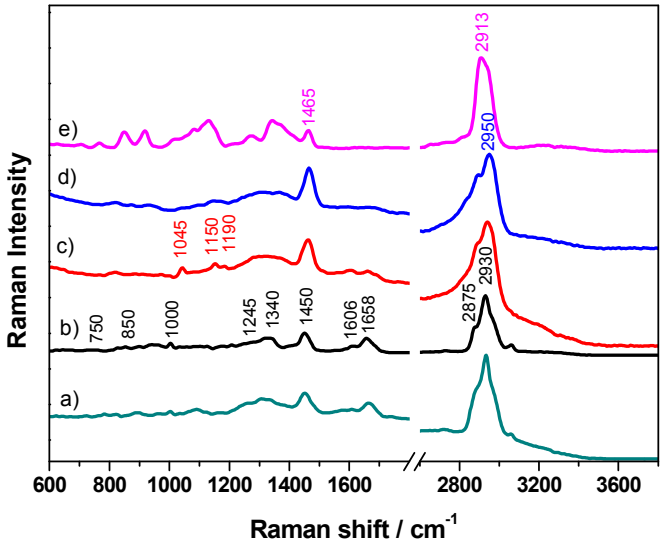

Figure 2. Raman spectra for (a) BTL2, (b) BSA, (c) the aminated dextran–BSA conjugate; (d) aminated dextran and (e) dextran.

The Raman spectra for BTL2 and BSA are typical of proteins,[29] with bands associated to the polypeptide backbone (Amide I, 1650 cm^{-1}), C–H deformation (1450 and 1341 cm^{-1}), Amide III (1240 cm^{-1}) and aromatic aminoacid (phenylalanine, tryptophan and tyrosine)[30] side chains.

In particular, the characteristic narrow band at 1000 cm^{-1} corresponds to the aromatic ring of phenylalanine and that at 1606 cm^{-1} to in-plane stretching of the ring.

A comparison of the Raman spectra for the aminated dextran and dextran revealed a red shift in the C–H stretching bands around 2900 cm^{-1}, an increased intensity in the C–H deformation band at 1465 cm^{-1}, and the presence of three new bands at 1190, 1150 and 1045 cm^{-1} typical of secondary amines.[21] There was also a small signal increase in the 3100–3400 cm^{-1} region, which typically contains amine N–H stretching vibration bands.

The Raman spectrum for the aminated dextran–BSA conjugates included the typical signals for the aminated dextran and weak bands typical of BSA (e.g., amide I at 1658 cm^{-1} and phenylalanine aromatic ring stretching at 1606 cm^{-1}). Therefore, the Raman data was also consistent with the formation of chimeras.

Surface functionalization. The sensor was constructed by immobilizing the conjugate onto glass planar waveguides. In theory, the interaction of the enzyme hydrophobic pocket with the glass surface would allow the dextran network to acquire an outward orientation facilitating further covalent coupling of MCLR.[31] Incubation of nonsilanized glass slides with aminated (6 kDa) dextran–BTL2 conjugates resulted in low sensitivity and poor reproducibility in the determination of MCLR, which was ascribed to the substrate hydrophilicity leading to low surface coverage. The silanizing agents HMDS, FOTS and DMDMS were tested to increase surface hydrophobicity. To this end, the resulting slides were incubated with the conjugates; this was followed by covalent immobilization of MCLR (30 μg mL^{-1}) as described in the Experimental Section (Figure 1Sb). The effect of the silanizing agent on biosensor sensitivity was evaluated via competitive inhibition assays involving incubating 0.2 μg mL^{-1} anti-MC Ab in the absence and presence of MCLR (1 μg L^{-1}), using DyLight649-labeled anti-mouse IgG (2.5 μg mL^{-1}) as revealing agent.

As can be seen in Figure 2S (Supporting Information), FOTS and HMDS coated surfaces exhibited the strongest fluorescence signals and highest sensitivity to MCLR. However, AFM characterization of the FOTS coated slides (Figure 3S.b in the Supporting Information) revealed

the formation of silane aggregates up to 50 nm high. This resulted in irreproducible conjugate immobilization and hence in poor immunoassay reproducibility.

Figure 3b shows a 1.5 × 1.5 μm^2 AFM topographic image of an HDMS-coated glass slide after incubation with BTL2 (0.5 mg mL^{-1}) for 30 min. The surface was covered by a homogeneous globular film similar to those typically observed in immobilized proteins[32] and having R_q = 0.74 nm.

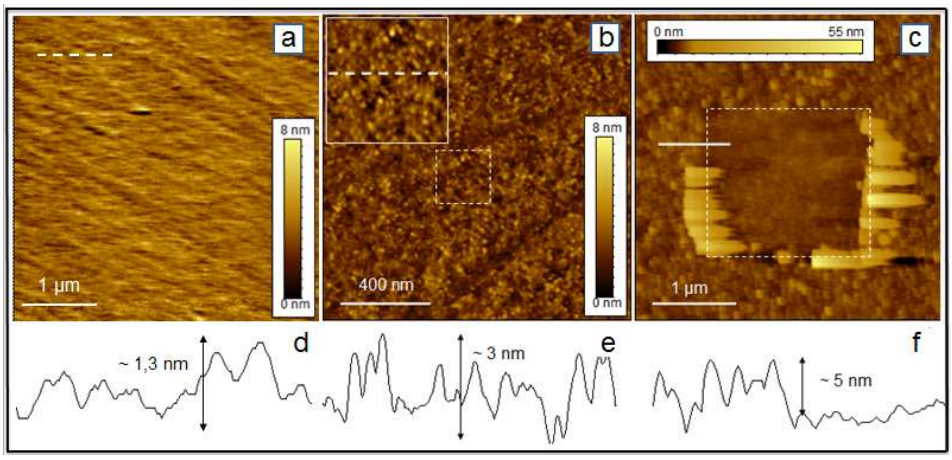

Figure 3. AFM topography of (a) a blank glass waveguide and (b) an HDMS silanized waveguide after incubation with a BTL solution (0.5 mg mL^{-1} in PB, 30 min). The inset corresponds to a zoom of the dashed square. (c) AFM topography image of an area that was previously scanned 20 times at a high load force in the contact mode. (d) Topographic profile across the line in Figure 3a. (e) Topographic profile across the line in Figure 3b. (f) Topographic profile across the line in Figure 3c.

The overall appearance of the BTL2-modified surface (Figure 3b) was markedly different from that of the bare glass (Figure 3a) or the HDMS-functionalized glass slides (Figure 3S.a in the Supporting Information), which was less rough —R_q was 0.42 for the former and 0.46 nm for the latter). This led us to select HMDS for waveguide silanization in subsequent tests. As suggested by the AFM results, BTL2 formed globules 1–3 nm high on the substrate in the HMDS-functionalized slides (see Figure 3e). Their R_q value, 0.74 nm, suggests the formation of

a lipase monolayer.[33] Based on the X-ray diffraction patterns for this protein, the expected height of the lipase globules was *ca.* 5 nm.[34] The decreased peak-to-hole distances measured in these samples can be ascribed to the formation of compact protein films preventing the AFM tip (close to 20 nm in diameter) from spanning the entire topography of the immobilized macromolecules (Figures 3b and 3e). The globules were 20–60 nm across, but this size was increased by effect of convolution with the AFM tip.[35]

An area of 2×2 μm^2 was scratched by repeated scanning in the contact mode with a high load force in order to further confirm the presence of a lipase monolayer. Scratching removed the material on top of the glass surface. A larger area containing the scratched zone was then scanned in the dynamic mode. The height of the resulting hole, shown in Figure 3c, was close to 5 nm (Figure 3f), which further confirms the presence of a lipase monolayer.

Immobilization of dextran–lipase conjugates onto planar waveguides. The immobilization procedure was optimized by examining the influence of the nature of the carrier solution, conjugate concentration and incubation time. Milli-Q water and two different buffers were used: PB (10–50 mM, pH 7.0) and TRIS (50 mM, pH 7.6) and the resulting surface morphology was characterized by AFM. The best results in terms of surface homogeneity were obtained with PB and water. Finally, a 10 mM PB solution at pH 7.0 containing 0.15 M NaCl was selected for the assay in order to reduce aggregation and increase conjugate solubility.[20,36]

The influence of the lipase concentration was examined over the range 0.5–1 mg mL^{-1}. After 30 min incubation, the AFM technique revealed the formation of homogeneous conjugate monolayers irrespective of the enzyme concentration used. As confirmed by AFM, longer incubation times produced no conjugate multilayers, which would have led to poor coating homogeneity and less uniform MCLR density across the waveguide surface. Therefore, the slides were incubated with a 0.5 mg mL^{-1} solution of aminated dextran–BTL2 conjugate dissolved in 10 mM PB (0.15 M NaCl, pH 7.0) for 30 min in subsequent tests. These experimental conditions facilitated the formation of a monolayer onto the silanized surface with good reproducibility between waveguides.

Effect of the dextran molecular weight on microarray sensitivity. Dextran networks of molecular weight spanning the range 1.5–40 kDa were bound to BTL2 in order to assess the effect of polysaccharide size on biosensor response. These polysaccharides are very flexible polymers that behave as expandable coils (Mw > 2000) in solution. A decrease in desorption yield of the aminated dextran–BTL2 conjugate from the octyl sephadex support with increasing dextran molecular weight was observed. The maximum yield was obtained with the 1.5 kDa dextran (40%); it was slightly lower for the 6 kDa dextran (37%) and reduced to about 16% with the 40 kDa oligosaccharide. This result can be ascribed to a single polysaccharide molecule binding to several lipase neighboring molecules to form complex conjugates which may not be so readily desorbed from the sepharose support as the molecular dimensions of the dextran network are increased.

Figure 4 shows 1 × 1 μm^2 topographic images of the immobilized aminated dextran–BTL2 conjugates containing polysaccharides of increasing molecular weight. R_q was 0.66, 1.23, 1.25, 1.33 and 1.64 nm for the 1.5 kDa, 6 kDa, 9–11 kDa, 15–25 kDa and 40 kDa dextran, respectively.

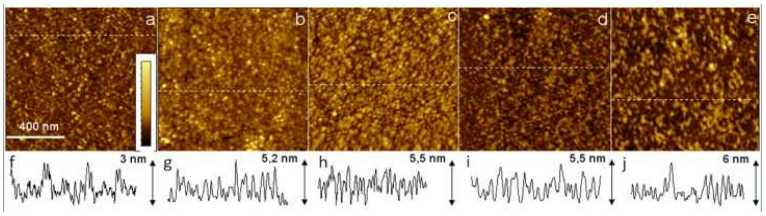

Figure 4. AFM topography images of an HDMS silanized waveguide coated with aminated dextran–BTL2 conjugates prepared from dextrans of variable molecular weight: (a) 1.5 kDa, (b) 6 kDa, (c) 9–11 kDa, (d) 15–25 kDa and (e) 40 kDa. Topographic profiles across the dashed lines drawn in a (f), b (g), c (h), d (i) and e (j). The topographic scale (inset) ranged from 0 to 9 nm.

The aminated (1.5 kDa) dextran–BTL2 conjugates (Figure 4a) and BTL2 (Figure 3b) had similar surface topographies, with globules 1–3 nm in size (Figure 4e) and R_q = 0.66 nm. This

result suggests that derivatization with the 1.5 kDa dextran had no significant effect on the enzyme dimensions, probably because of the relatively small size of the attached oligosaccharide. Immobilizing polysaccharide derivatives of higher molecular weights (6, 9–11 and 15–25 kDa) also led to homogeneously modified surfaces with globules up to 5 nm high (Figures 4g, 4h and 4i).

The topography of the sample corresponding to the waveguide surface after incubation with an aminated (40 kDa) dextran–BTL2 conjugate was markedly different from those of the other substrates (Figure 4e). Globules ranged from 1 to 6 nm in height (Figure 4j) and the intervening space exceeded 60 nm. Also, R_q increased to 1.64 nm. These results may have arisen from the increased molecular volume of the dextran molecules potentially coming into contact with neighboring dextrans and aggregating laterally to form higher, more spaced globules.

The aminated dextran-BTL2 patterned slides were incubated with MCLR (30 μg mL^{-1}) in MES buffer containing 100 mM EDC and 50 mM NHS to perform the competitive inhibition assays. No changes in surface topography were observed by AFM after covalent binding of MCLR to the aminated (6 kDa) dextran–BTL2 conjugate (results not shown). After incubation with anti-MC Ab (Figure 5a), the surface exhibited globules 12–22 nm high and 70–150 nm wide (see profiles in Figure 5b). These dimensions are similar to those of an IgG molecule and the slight differences are suggestive of a different orientation in the Ab molecules. R_q between Ab globules was 1.10 nm, and scratching the surface produced a 5 nm deep hole; both are consistent with the presence of a conjugate monolayer (result not shown).

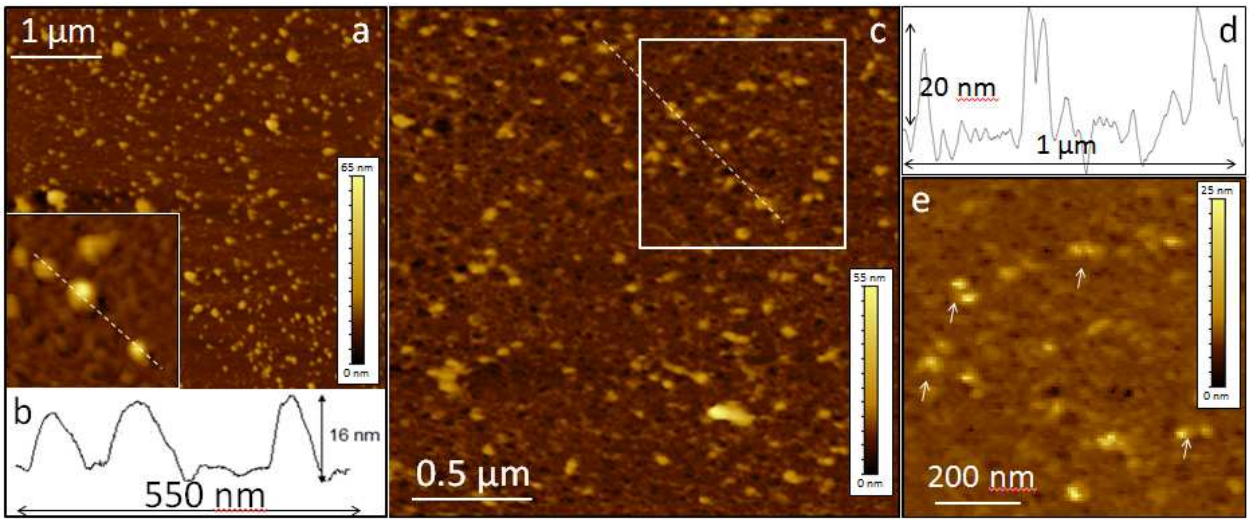

Figure 5. (a) AFM topography image of the MCLR-(6 kDa) dextran–BTL2 sensor surface after incubation with anti-MC Ab (1 µg mL^{-1}, 20 min). The inset is a 500 × 500 nm^2 zoom of the sample. (b) Topographic profile following the dashed line in the inset. (c) AFM topographic image of the waveguide surface after the revealing step. (d) Topographic profile following the dashed line; (e) 0.8 × 0.8 μm^2 zoom of the square in (c). The arrows indicate the presence of globule pairs.

Figure 5c shows a topographic image of the sensing surface after the revealing step with labeled Ab. An increased number of globules and other variously shaped objects 16–20 nm high and 60 to a few hundred nanometers wide were observed (Figure 5d). Zooming on the surface revealed a large number of globules in pairs (Figure 5e) about 20 nm in height and 150 nm in total width that were assigned to secondary fluorescent antibodies bound to anti-MC.

Probably, the wider structures observed were protein aggregates or reflected different orientations of the labeled antibodies upon binding. The surface also contained several holes 5 nm in average height suggestive of unbound MCLR-dextran–BTL2 conjugates. Again, scratching the surface produced a hole nearly 5 nm deep that confirmed the presence of a conjugate monolayer under the antibodies (results not shown).

A control assay was conducted in parallel by directly adsorbing MCLR onto the HDMS functionalized surface (Figure 4S in the Supplementary Material). AFM revealed no significant

changes after cyanotoxin immobilization. However, incubation with anti-MC Ab led to a disordered surface of polydisperse globules ranging from 10 to more than 100 nm in height (Figure 4S.a). Further incubation with labeled secondary Ab again rendered a disordered topography (Figure 4S.b) with aggregates up to 140 nm high (Figure 4S.d).

Replacing the BTL2 conjugates with MCLR-aminated (6 kDa)-dextran for slide patterning also resulted in highly disordered surfaces after incubation with anti-MC Ab (Figure 5S.a.) and after revealing with labeled secondary Ab (Figure 5S.b).

The lack of homogeneity observed confirms the suitability of dextran–BTL2 conjugates for preparing highly ordered molecular architectures for further immobilization of low molecular weight haptens on planar waveguides.

The effect of polysaccharide molecular weight on microarray sensitivity was assessed via competitive inhibition assays with toxin concentrations over the range 0–1 µg mL^{-1}. The resulting IC_{50} values and LODs are shown in Table 1S and Figure 6, and were significantly lower ($P < 0.0001$, unpaired Student's *t*-test) than those obtained with the aminated (6 kDa) dextran functionalized glass slides (Table 2S, IC_{50}: 0.81 ± 0.04 µg L^{-1}).

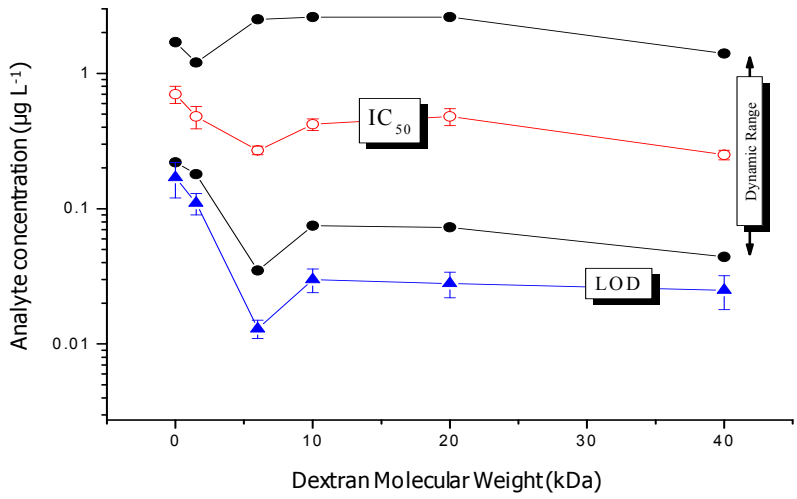

Figure 6. Influence of dextran molecular weight on microarray sensitivity. Solid black circles represent the DR upper and lower boundaries, open red circles IC_{50} values and blue triangles LODs (see Table 1S).

As can be seen, the optimum dextran molecular weight was 6 kDa, which led to the broadest dynamic range by far —and also to the lowest LODs and IC_{50} values as a result.

In order to elucidate the mechanism underlying this phenomenon, we fitted the response curves for each molecular weight to a physical model describing the binding mechanism. Specifically, we used the Sips equation[37] to determine the Sips parameter, which is a measure of 3D binding. A detailed discussion of the Sips equation and the significance of the Sips parameter in differentiating between 2D and 3D binding is provided as supplementary information. A brief description follows. The equation for binding inhibition assays and normalized data (our case) was as follows:

$$Y = 1 - \left(\frac{c}{k + c} \right)^{\alpha} \qquad (2)$$

where Y is the fraction of bound analyte, c the analyte concentration in solution, k the dissociation coefficient and α the Sips parameter. It should be noted that, with $\alpha = 1$, eq. (2) converges to the Langmuir equation, which describes ideal monolayer adsorption of the analyte. With $\alpha < 1$, the equation describes an accumulation mechanism similar to that of adsorption of the analyte in the third dimension (depth), *i.e.*, a layer with a finite —however small— thickness as opposed to a monolayer.[38]

Figure 6S in the Supplementary Material summarizes these results as a plot of extracted α against dextran molecular weight. With molecular weights below 6 kDa (*i.e.*, no dextran or 1.5 kDa dextran), $\alpha = 1$ and a pure 2D binding mechanism can be assumed. At higher dextran molecular weights, α was considerably lower, with a minimum (0.5) at 6 kDa. The striking resemblance of the behavior of α (Figure 6S) to those of LOD, IC_{50} and DR (see Table 1S and Figure 6) leads to the following conclusion: modification with longer dextran chains creates a three-dimensional surface, thereby effectively increasing the loading capacity by effect of the analyte binding deeply in the surface and leading to a broader DR, and to lower LOD and IC_{50} values. Based on the foregoing, we chose to use the 6 kDa dextran to prepare the microarray.

Bioassay optimization. The effect of the MCLR concentration in the patterning solution was evaluated over the range 5–30 μg mL^{-1}. Increasing the MCLR concentration up to 20 μg mL^{-1} increased signal intensities. Concentrations above this level failed to significantly improve biosensor response, however. A 20 μg mL^{-1} concentration of MCLR was thus selected for further testing. Such a low concentration should allow the cost per assay to be significantly reduced with respect to previous developments.[13,14] The effect of the anti-MC Ab concentration was studied over the range 0.05–0.3 μg mL^{-1} and 0.1 μg mL^{-1} found to provide the lowest IC_{50} and LOD values, thus being selected as optimal.

The IC_{50} and LOD values obtained under the above-described optimum conditions were 4.4 ± 0.7 ng L^{-1} (n = 9) and 0.007 ± 0.001 ng L^{-1} (n = 9), respectively; also, DR was 0.09–136.56 ng L^{-1}. The proposed biosensor exhibits substantially increased sensitivity relative to most existing immunosensors applied to the analysis of MCLR in water samples with limits of detection in the range 16–10^3 ng L^{-1}.[13,14,39–43]

Reproducibility within slide channels was good (RSD for the normalized signal ranged from 5 to 15% depending on the particular MCLR concentration). Slide to slide reproducibility in the competitive immunoassay (3 slides per run) was also good, with RSD ≤ 23% —the mean RSD in the calibration range was 16 %. Long term sensor stability was assessed by measuring the fluorescence intensity in the absence and presence of 10 ng L^{-1} MCLR under the optimum conditions. As shown in Figure 7S, no significant differences at the 95% confidence level in biosensor response were observed over a period of 10 days after preparation of the waveguides. Moreover, changes in biosensor response after at least 10 assay regeneration cycles—the maximum number studied— were negligible and differences in the signal in the absence of MCLR were not statistically significant at the 95% confidence level.

Cross-reactivity in terms of the IC_{50} ratio of MCLR to each potentially interfering compound was examined for the three MC variants most commonly encountered in freshwater samples apart from MCLR[44] and found to be 92%, 98% and 88% for MCRR, dm-MCRR and MCYR, respectively. Because Ab recognizes [4-arginine]-MCs with a similar sensitivity,[45] our

biosensor allows the total concentration of the most common MCs in environmental water samples to be quantified.

Finally, the microarray was applied to the determination of MCLR in tap water samples in order to assess its analytical performance. The samples were previously checked for containing undetectable amounts of MCLR. No matrix effect was observed when the dose-response curve was obtained in tap water, instead of ultrapure Millie-Q water. As shown in Table 1 good recoveries were achieved for the analyzed samples thus demonstrating the potential of the microarray for the direct determination of the cyanotoxin at levels far below the provisional guideline value for drinking water proposed by WHO (1 μg L^{-1} for MCLR), without further sample cleanup and pre-concentration.

Table 1. Recoveries for MCLR-spiked tap water samples (n = 6).

Spiked MCLR μg L^{-1}	Detected concentration μg L^{-1}	Recovery (%)
0.01	0.011 ± 0.003	110%
0.1	0.08 ± 0.02	80%

± ts/√n, 95% confidence limit

CONCLUSIONS

As confirmed by AFM imaging, dextran–BTL2 conjugates are effective for preparing highly ordered and homogeneous molecular architectures on planar waveguide substrates. As also confirmed by AFM, these chimeras can be further functionalized with low molecular weight haptens such as MCLR without compromising the stability of the conjugate monolayer. These platforms can be used to develop immunosensor arrays for fluorescence measurements. Surface modification with conjugates bearing dextrans with molecular weights ≥ 6 kDa provides a three-dimensional layer, thereby effectively increasing the loading capacity by effect of the analyte binding to the polymeric structure as opposed to the surface alone and hence leading to a broader DR, and lower LODs and IC_{50} values, in immunoassays.

Research into the potential use of this approach for preparing multianalyte microarrays for detecting low molecular weight molecules including patterning slides with dextran–BTL2 conjugates previously functionalized with the desired hapten is currently under way. This strategy provides an alternative approach to controlling surface functionalization with a view to preparing high density receptor layers on glass microscope slides largely independent of surface morphology.

ASSOCIATED CONTENT

Supporting Information. Analytical performance of microarrays prepared by patterning MCLR or MCLR-dextran–BTL2 conjugates of variable molecular weight on planar waveguides; Scheme of the synthesis of dextran–BTL2 conjugates and waveguide functionalization; Effect of silane functionalization of the planar waveguide on biosensor response; AFM topography of nonsilanized and glass waveguides; AFM topography of an HMDS functionalized waveguide patterned with MCLR during the immunoassay steps; Sips parameter (α) as a function of dextran molecular weight; Variation of the evanescent field intensity and layer thickness as a function of the distance from the glass support. This material is available free of charge via the Internet at http://pubs.acs.org.

AUTHOR INFORMATION

Corresponding Authors

mcmbondi@quim.ucm.es; jmguisan@icp.csic.es

ACKNOWLEDGMENTS

This work was funded by Spain's Ministry of Education and Science (Project CTQ2009-43014565-C03) and Complutense University (GR35/10-A). S. Herranz thanks the Madrid Regional Government for award of a PhD contract. D.O. acknowledges the JAE program of CSIC and the European Social Fund.

REFERENCES

(1) Donhauser, S. C.; Niessner, R., Seidel, M. *Anal. Chem.* **2011**, *83*, 3153.

(2) Arrabito, G.; Pignataro, B. *Anal. Chem*. **2012**, 84, 5450.

(3) Dill, D.; Hui Liu, R.; Grodzinski, P. (Eds.) *Microarrays. Preparation, Microfluidics, Detection Methods, and Biological Applications.* Springer Science, New York, **2009**.

(4) North, S. H.; Lock, E. H.; King, T. R.; Franek, J. B.; Walton, S. G.; Taitt, C. R. *Anal. Chem*. **2010**, *82*, 406.

(5) Wu, H.; Ge, J.; Uttamchandani, M.; Yao, S. Q. *Chem. Commun*., **2011**, *47*, 5664.

(6) Valles-Miret, M.; Bradley, M. *Tetrah. Lett.* **2011**, *52*, 6819.

(7) Miller, J. C.; Zhou, H.; Kwekel, J.; Cavallo, R.; Burke, J.; Butler, E. B.; Teh B. S.; Haab, B. B. *Proteomics* **2003**, *3*, 56.

(8) Ramakrishnan, R.; Dorris, D.; Lublinsky, A.; Nguyen, A.; Domanus, M.; Prokhorova, A; Gieser, L.; Touma, E.; Lockner, R.; Tata, M.; Zhu, X.; Patterson, M.; Shippy, R.; Sendera T. J.; Mazumder, A. *Nucleic Acid Res*. **2002**, *30*, e30.

(9) Afabassiev, V.; Hanemann, V.; Wölfl, S. *Nucleic Acid Res.* **2000**, *28*, e66.

(10) Koch, C. A.; Li, P. C. H.; Utkhede, R. S. *Anal. Biochem.* **2005**, *342*, 93.

(11) Löfås, S.; Mcwhirter, A. *Springer Ser. Chem. Sensors Biosens.* **2006**, 4, 117.

(12) Gesellchen, F.; Zimmermann, B.; Herberg F. W. *Direct Optical Detection of Protein–Ligand Interactions* in *Protein Ligand interactions. Methods and applications*. Nienhaus G. U. (Ed.), Humana Press, Totowa (NJ), **2005**.

(13) Herranz, S.; Bocková, M.; Marazuela, M. D.; Homola, J.; Moreno-Bondi, M. C. *Anal. Bioanal. Chem.* **2010**, *398*, 2625.

(14) Herranz, S.; Marazuela M. D.; Moreno-Bondi, M. C. *Biosens. Bioelectron.* **2012**, *33*, 50.

(15) Feldstein, M. J.; Golden, J. P.; Rowe, C. A.; MacCraith, B. D.; Ligler, F. S. *Biomed. Microdevices* **1999**, *1*, 139.

(16) Ligler, F. S.; Sapsford, K. E.; Golden, J. P.; Shriver-Lake, L. C.; Taitt, C. R.; Dyer, M. A.; Barone, S.; Myatt, C. J. *Anal. Sci.* **2007***, 23,* 5.

(17) Schmidt-Dannert, C.; Rúa, M. L.; Atomi, H.; Schmid, R. D. *Biochim. Biophys. Acta* **1996**, *1301*, 105.

(18) Marciello, M.; Mateo, C.; Guisán, J. M. *Colloids Surf., B* **2011**, *84*, 556.

(19) Carrasco-López, C.; Godoy, C.; de las Rivas, B.; Fernández-Lorente, G.; Palomo, J. M.; Guisán, J. M.; Fernández-Lafuente, R.; Martínez-Ripoll, M.; Hermoso, J. A. *J. Biol. Chem.* **2009**, *284*, 4365.

(20) Hermanson, G. T. *Bioconjugate Techniques*. 2nd ed., Academic Press, USA, **2008**.

(21) Socrates, G. *Infrared and Raman Characteristic Group Frequencies: Tables and Charts.* 3rd ed., Wiley and Sons, Chichester, **2001**.

(22) http://webbook.nist.gov/chemistry/

(23) Dumitrascu, M.; Meltzer, V.; Sima, E.; Virgolici, M.; Albu, M. G.; Ficai, A.; Moise, V.; Minea, R.; Vancea, C.; Scarisoreanu, A.; Scarlat, F. *Dig. J. Nanomater. Bios.* **2011**, *6*, 1793.

(24) Ombelli, M.; Eckmann, D. M.; Composto, R. J. *MRS Proceedings* **2003**, *774*, O7.25.

(25) Maia, J.; Ferreira, L.; Carvalho, R.; Ramos, M. A.; Gil, M. H. *Polymer* **2005**, *46*, 9604.

(26) Tan, H.; Hu, X. *J. Appl. Polym. Sci.* **2012**, *126*, E180.

(27) Trott, G. F.; Woodside, E. E. *J. Colloid Interf. Sci.* **1971**, *36*, 40.

(28) Natalello, A.; Ami, D.; Brocca, S.; Lotti, M.; Doglia, S. M. *Biochem. J.* **2005**, *385*, 511.

(29) Tuma, R. *J. Raman Spectrosc.* **2005**, *36*, 307.

(30) Fischer, W. B.; Eysel, H. H. *Spectrochim. Acta A* **1992**, *48*, 725.

(31) Palomo, J. M.; Segura, R. L.; Fernández-Lorente, G.; Pernas, M.; Rua, M. L.; Guisán, J. M.; Fernández-Lafuente, R. *Biotechnol. Prog.* **2004**, *20*, 630.

(32) Laszlo, J. A.; Evan, K. O. *J. Mol. Catal. B: Enzym.* **2007**, *48*, 84.

(33) Kosaka, P. M.; Kawano, O. A.; El Seoud, O. A.; Petri, D. F. S. *Langmuir* **2007**, *23*, 12167.

(34) Carrasco-López, C.; Godoy, C.; De las Rivas, B.; Fernández-Lorente, G.; Palomo, J. M.; Guisan, J. M.; Fernández-Lafuente, R; Martínez-Ripoll, M.; Hermoso, J. A. *Acta Cryst.* **2008**, *F64*, 1043.

(35) Markiewicz, P.; Goh, M. C. *J. Vac. Sci. Technol. B* **1995**, *13*, 1115.

(36) Rúa, M. L.; Schmidt-Dannert, C.; Wahl, S.; Sprauer, A.; Schmid, R. D. *J. Biotechnol.* **1997**, *56,* 89.

(37) Sips, R. *J. Chem. Phys.* **1948**, *16*, 490.

(38) Tsarfati–BarAd, I.; Sauer, U.; Preininger, C.; Gheber, L. A. *Biosens. Bioelectron.* **2011**, *26*, 3774.

(39) Hu, C.; Gan, N.; Chen, Y.; Bi, L.; Zhang, X.; Song. L *Talanta* **2009**, *80,* 407.

(40) Lindner, P.; Molz, R.; Yacoub-George, E.; Wolf, H. *Anal. Chim. Acta* **2009**, *636,* 218.

(41) Ma, W.; Chen, W.; Qiao, R.; Liu, C.; Yang, C.; Li, Z.; Xu, D.; Peng, C.; Jin, Z.; Xu, S.; Wang, L. *Biosens. Bioelectron.* **2009**, *25,* 240.

(42) Tippkötter, N.; Stückmann, H.; Kroll, S.; Winkelmann, G.; Noack, U.; Scheper, T.; Ulber, R. *Anal. Bioanal. Chem.* **2009**, *394,* 863.

(43) Yu, H. W.; Lee, J.; Kim, S.; Nguyen, G. H.; Kim, I. S. *Anal. Bioanal. Chem.* **2009**, *394,* 2173.

(44) Sivonen, K., Jones, G. *Toxic cyanobacteria in water: A guide to their public health consequences, monitoring and management.* Chorus, I., Bratram, J. (Eds.); E & F.N. Spon, London, **1999**, Chpt 3, p. 41.

(45) Zeck, A.; Eikenberg, A.; Weller, M. G.; Niessner, R. *Anal. Chim. Acta* **2001**, *441,* 1.

For TOC only

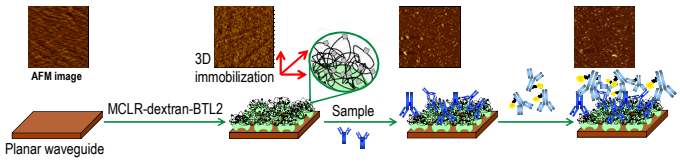
AFM image
3D
immobilization
MCLR-dextran-BTL2
Sample
Planar waveguide